Journal of Environmental Management 265 (2020) 110514

Contents lists available at ScienceDirect

Journal of Environmental Management

journal homepage: http://www.elsevier.com/locate/jenvman

Research article

Carbon and phosphorus transformation during the deposition of particulate matter in the large deep reservoir

Jia Yu [a,b], Jingan Chen [a,**], Yan Zeng [a,*], Yaoting Lu [a,b], Quan Chen [a,b]

[a] State Key Laboratory of Environmental Geochemistry, Institute of Geochemistry, Chinese Academy of Sciences, Guiyang, 550081, PR China
[b] University of Chinese Academy of Sciences, Beijing, 101408, PR China

ARTICLE INFO

Keywords:
Carbon
Phosphorus
Organic matter degradation
Particulate matter
Large deep reservoir

ABSTRACT

As the running time of reservoirs is increasing, a large number of reservoirs are becoming eutrophicated. Organic phosphorus (OP) is a key factor in eutrophication. However, the mechanism and extent to which organic matter degradation affects P recycling in water column of large deep reservoirs are unclear, especially for the newly-built ones. In this study, different forms of carbon (C) and P in the water column of Hongjiadu Reservoir were investigated. The contents of particulate organic carbon (POC) and particulate organic phosphorus (POP) both decreased with depth in summer, indicating that organic matter was degraded during the deposition of particulates. In contrast, the contents of POC and POP varied slightly with depth in winter. This difference may result from the double thermal stratification and the corresponding double oxygen stratification in summer. The POC/POP ratios were lower in the epilimnion and increased with depth, suggesting that P was preferentially regenerated relative to C during organic matter degradation. The contents of particulate inorganic phosphorus (PIP) and POP were significantly negatively correlated, indicating that POP transformed into PIP in deeper water. The double thermoclines and oxyclines in Hongjiadu Reservoir lead to very low dissolved oxygen (DO) concentrations in the hypolimnion, which should receive sufficient attention. If water becomes hypoxic, enhanced P release during organic matter degradation will promote phytoplankton growth, leading to higher phytoplankton biomass and more severe DO depletion. Thus, a positive feedback loop may form among hypoxia, enhanced P release, higher primary productivity, and more severe hypoxia, accelerating P recycling in large deep reservoirs. Once if eutrophication occurs in these reservoirs, it will be very difficult to restore the water ecosystem. Thus, it is particularly important to prevent the occurrence of eutrophication and the formation of positive feedback loop as early as possible. This highlights the importance of both reducing external loading and improving DO level in large deep reservoirs.

1. Introduction

In the past century, high numbers of dams have been constructed on rivers for supplying drinking water, generating power, flood control, irrigation, recreation, and aquaculture (Gao et al., 2013). Although these hydrological landscapes have provided many societal benefits, dams have also altered the riparian ecosystem, including both the physical structure of the river system and nutrients transport, causing nutrients to be retained in reservoir (Bao et al., 2018; Wang et al., 2019a). Maavara et al. (2015) estimated that approximately 42 Gmol y^{-1} of total phosphorus (TP) was trapped by dammed reservoirs in 2000. In addition, the storage of water has decreased the oxygen concentration at the water-sediment interface, which might lead to nutrient release from sediments in large deep reservoirs (Wang et al., 2012).

Phytoplankton fixes dissolved inorganic carbon (DIC) and soluble reactive phosphorus (SRP) to form organic matter such as carbohydrates, phospholipids, and nucleotides (Van Mooy et al., 2009). The fixed C and P are preserved as organic matter and sink into sediments (Chen and Liu, 2017). During deposition, parts of endogenous organic matter is degraded, leading to the release of C and P into water (Yan et al., 2018). Han et al. (1994) estimated that 35% of POC generated by primary production was mineralized and recycled in the euphotic layer. Other exogenous particulates also decompose and release nutrients to water column, although they are recalcitrant (Reitzel et al., 2007).

* Corresponding author.
** Corresponding author.
E-mail addresses: chenjingan@vip.skleg.cn (J. Chen), zengyan@vip.skleg.cn (Y. Zeng).

https://doi.org/10.1016/j.jenvman.2020.110514
Received 25 December 2019; Received in revised form 10 March 2020; Accepted 27 March 2020
Available online 7 April 2020

Roden et al. (1995) reported that approximately 36%–74% of POC could be deposited to sediment in the mesohaline Chesapeake Bay, indicating that approximately 26%–64% of POC decomposed in water column. POC mineralization would release greenhouse gases, such as CO_2 and CH_4 to the atmosphere, and the regeneration of P from particulates is also considerable (Maavara et al., 2020). Chen et al. (2019) suggested that approximately 25.1 ± 9.0 t P could be released from sestons and sediments each year in the Hongfeng Lake, and increasing numbers of studies have suggested that OP is a key factor in eutrophication (Ahlgren et al., 2005; Wu et al., 2010; Baldwin, 2013; Joshi et al., 2015). OP contains many labile species, and the degradation of OP releases phosphate, which could be directly assimilated by organisms (Rydin, 2000; Zhu et al., 2018). Therefore, particulate matter plays an important role in C and P cycling in the aquatic ecosystem, particularly for the large deep reservoir/lake, where particulates retain in water column for a longer period.

Lots of studies have focused on the activation of particulate C and P in the marine ecosystem (Knauer et al., 1979; Jilbert et al., 2011; Dijkstra et al., 2018). However, there have been relatively few investigations of large deep reservoirs (He et al., 2009), especially for the newly-built oligotrophic ones. The mechanism and extent to which organic matter degradation during precipitation of particulates affects P recycling in water column of large deep reservoirs remain unclear. Therefore, in this study, we selected Hongjiadu Reservoir, a typical large and deep reservoir constructed in 2004, to investigate the transformation of C and P during the deposition of particulates in water column with the aim to provide guidance for formulating effective strategies on eutrophication control in large deep reservoirs.

2. Materials and methods

2.1. Study region

Hongjiadu Reservoir is located in the suburb of Bijie City, Guizhou Province in southwest of China (Fig. 1). It is a cascade reservoir situated at the upstream of Wujiang River, the largest tributary of the Yangtze River on the right bank. Two rivers feed the reservoir. The largest one is Liuchong River (total length: 268 km, catchment area: 10665 km^2), which is the largest tributary of Wujiang River (Li et al., 2019b). The other one is Aushui River. The catchment area of Hongjiadu Reservoir is 9940 km^2, and the total volume is 49.25 × 10^8 m^3. The normal and dead storage levels are 1140 and 1076 m, respectively, and the average residence time is 368.8 d (Liu et al., 2011; Xiang et al., 2016). The maximum water depth is > 120 m. The whole catchment is enriched in limestone. The topography of the reservoir is characterized as long and narrow, and the pollution sources are mainly river inputs. Hongjiadu Reservoir was constructed in 2004 and is still oligotrophic.

2.2. Sampling

Water samples were collected at six representative sites using a Niskin sampler in August 2017 and January 2018 (Fig. 1, Table 1). The temperature (T), pH, DO and chlorophyll-a (Chl-a) were monitored *in situ* using an automated multi-parameter instrument (YSI 6600 V2). The water transparency was measured using a Secchi disk. Combined with the data from YSI, we sampled water from the epilimnion (3 m), the middle layer (45–55 m) and the hypolimnion (90–120 m) at each site. Some water samples were filtered on-board with a stainless steel canister and pre-combusted (450 °C,3h) and pre-weighed glass-fiber membranes (0.70 μm, Whatman GF/F). The filtrates were collected in glass bottles for the analysis of DIC and dissolved organic carbon (DOC), and the filter samples were packed in pre-combusted (450 °C,3 h) aluminum foil to analyze the particulate C and P contents. Some water samples were filtered through acetate-fiber membranes in lab. The filtrates were collected in polyethylene bottles for the analysis of dissolved nutrient contents, and the filter samples were collected at the Site 2 and Site 5 for measuring the contents of particulate metals. Bulk water samples without any filtration were used to analyze total phosphorus (TP). All liquid samples were stored at 4 °C, and all filter samples were stored at −20 °C until analysis.

2.3. Measurements of TP and dissolved C, N, and P

The concentration of DOC was measured using a total organic carbon analysis instrument (Elementar-Vario TOC select). As the pH of Hongjiadu Reservoir ranged from 7.5 to 9.6, HCO_3^- was the primary component of DIC. An alkalinity titration test kit was used to measure the concentration of HCO_3^- *in situ*, which represented the content of DIC. The total dissolved nitrogen (TDN) content was determined following the alkaline potassium persulfate digestion-UV spectrophotometric method, while nitrate-nitrogen (NO_3^--N) and ammonia-nitrogen (NH_4^+-N) were measured by ion liquid chromatography and Nessler's reagent spectrophotometry, respectively. The SRP content was determined following the colorimetric molybdenum blue method, while the content of total dissolved phosphorus (TDP) was determined by potassium persulfate digestion, followed by the same method as SRP. The TP content was determined following the same method as TDP without filtration. Three parallel samples were measured at the intervals of 5 samples for all of these analysis. The results of the parallel sample analysis showed that relative standard deviations (RSD) were less than 5% and 3% for DOC and DIC, less than 4%, 2% and 6% for NH_4^+-N, NO_3^--N and TDN respectively, and less than 10% for TP. Almost all the results of the determination of SRP and TDP were below detectable limits.

2.4. Measurements of particulate C and N

After freeze-drying, the filter samples were weighed again to calculate the particulate mass. The particulate total carbon (PTC) content was measured using an element analyzer (Elementar-Vario MACRO cube), POC and the particulate nitrogen (PN) contents were measured using the same instrument following vapor acidification (Hedges and Stern, 1984; Komada et al., 2008). The particulate inorganic carbon (PIC) content was determined by the difference between the contents of PTC and POC. Because of the inhomogeneity of the particulates in the membranes, each sample was measured at least in triplicate to ensure that the RSD of every sample was less than 10%, and the mean values were reported.

2.5. POP and PIP determination

The particulate phosphorus fraction was measured following the Standards Measurements and Testing Program (SMT). The particulate total phosphorus (PTP) was determined by 3.5 mol L^{-1} HCl extraction (16 h) after ashing at 500 °C in a resistance furnace for 2 h. PIP content was determined by 1 mol L^{-1} HCl extraction (16 h) without ashing. Both extracted solutions were neutralized in 4 mol L^{-1} NaOH, and the concentrations were measured with the colorimetric molybdenum blue method. POP content was calculated as the difference between the contents of PTP and PIP (Aspila et al., 1976). Each sample was also measured at least in triplicate, and the average values were reported with the RSD less than 10%.

2.6. Measurement of particulate Al, Zr, Fe, and Mn

Site 2 and Site 5 were selected for the analysis of the particulate metal contents, because the samples of the two sites can roughly reflect the characteristics of inflow water and inlake water respectively. As shown in Fig. 1, Site 2 is located near the estuary of Aushui River, while Site 5 is located at the center of the whole reservoir.

The lyophilized acetate-fiber membranes were weighed again to determine the particulate mass. Particulate samples were digested in nitric (HNO_3), hydrofluoric (HF) and perchloric ($HClO_4$) acid. The digested samples were diluted to 100 mL with deionized water.

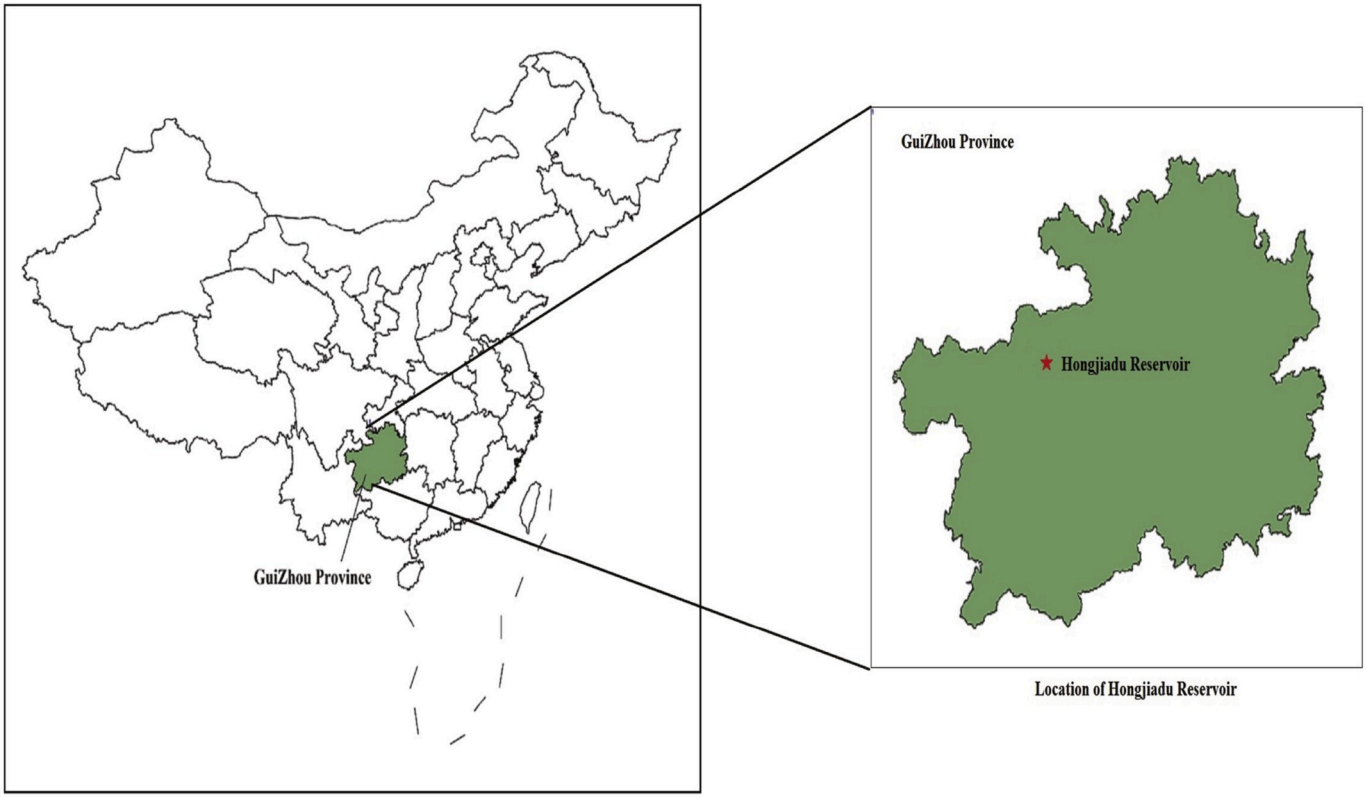

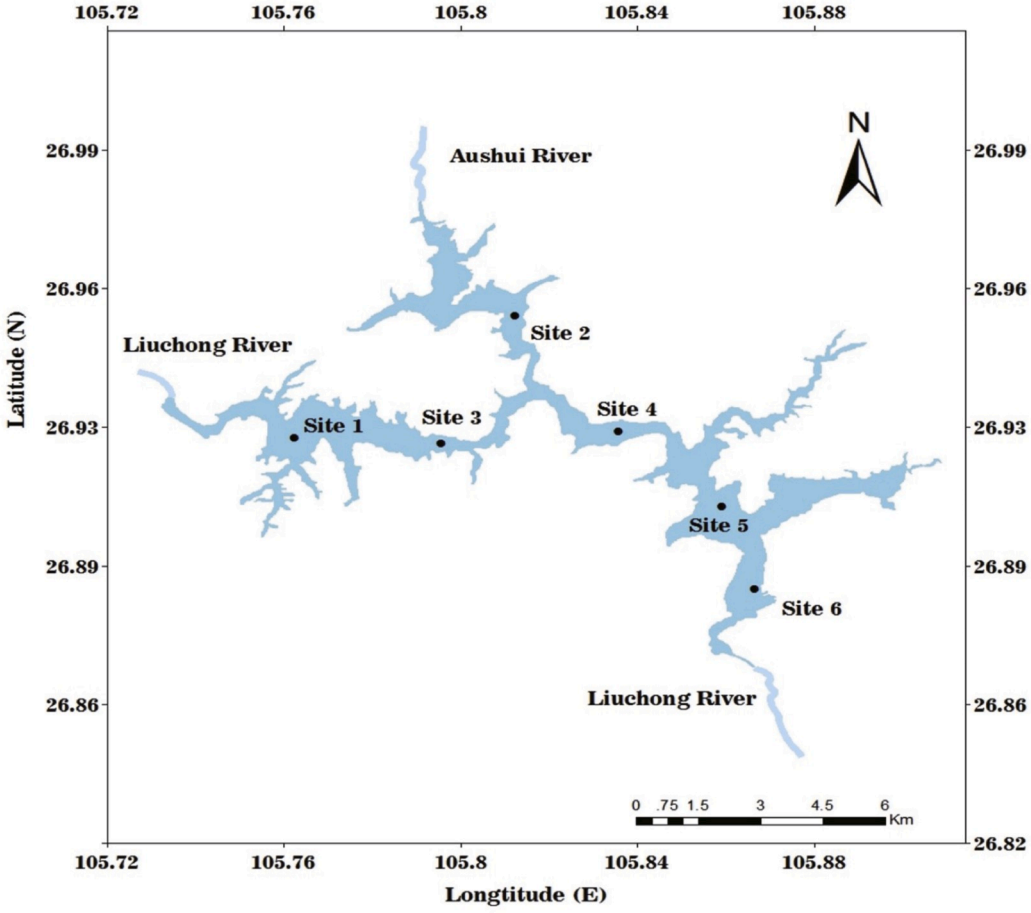

Fig. 1. Map of the sampling sites in Hongjiadu Reservoir. Site 6 was located in front of the dam of Hongjiadu Reservoir.

Table 1
Sampling sites description of latitude, longitude and sampling depth in Hongjiadu Reservoir.

	Latitude (N)	Longitude (E)	Epilimnion (m)	Middle layer (m)	Hypolimnion (m)
Site 1	26°55′31″	105°45′49″	3	55	100
Site 2	26°57′20″	105°48′01″	3	50	90
Site 3	26°55′20″	105°46′30″	3	45	100
Site 4	26°55′18″	105°50′08″	3	45	90
Site 5	26°54′21″	105°51′29″	3	55	120
Site 6	26°53′07″	105°51′54″	3	55	120

Inductively coupled plasma mass spectrometry (ICP-MS) was used to determine the contents of aluminum (Al), zirconium (Zr), iron (Fe) and manganese (Mn). The systemic error was below ±5%, with 95%–105% recovery.

3. Results

3.1. Physical and chemical parameters in water column

The profiles of the physical and chemical parameters in water column exhibited thermal stratification in August 2017, and vertical mixing in January 2018, respectively (Fig. 2a and b). Two thermoclines (water layer where the temperature gradient is > 0.2 °C m^{-1}) appeared in August 2017. The first thermocline occurred in the euphotic zone (5–15 m), where the temperature decreased from 26 °C to approximately 19 °C. The second thermocline occurred between 55 and 65 m, where the temperature decreased from 16 °C to approximately 13 °C. The pH also decreased sharply in the first thermocline and then declined gradually with depth (Fig. 2c). The contents of DO and Chl-a both increased from the surface and peaked in the upper layer of the first thermocline, and then decreased sharply. The DO content declined rapidly again in the second thermocline (Fig. 2e and g). In the mixing period, the temperature and Chl-a content in the surface water were significantly lower than those in August 2017, and these parameters all varied slightly in the vertical direction (Fig. 2b,2d,2f,2h). The water transparency was 3.1–4.6 m in the stratification period, and 5.4–6 m in the mixing period.

3.2. Concentrations of C, N, and P in water column

The concentrations of DOC and DIC varied from 0.68 to 1.73 mg L^{-1} and 19.2–31.2 mg L^{-1} in August 2017, respectively, while they varied from 1.45 to 4.32 mg L^{-1} and 27.6–34.8 mg L^{-1} in January 2018, respectively. Generally, DIC was the dominant dissolved carbon fraction. The DOC concentration decreased with depth, while the DIC concentration exhibited an opposite trend in August 2017. The DIC concentration varied slightly in vertical direction in January 2018. Furthermore, the concentrations of DOC and DIC were both much higher in January than in August (Fig. 3a–d).

The concentrations of TDN, NO_3^--N, and NH_4^+-N varied from 3.43 to 6.81 mg L^{-1}, 3.25–5.22 mg L^{-1}, and 0.03–0.72 mg L^{-1} in August 2017, respectively, while they varied from 2.90 to 4.75 mg L^{-1}, 1.82–3.65 mg L^{-1}, and 0.02–0.27 mg L^{-1} in January 2018, respectively (Fig. 3e–j). TDN consisted mainly of NO_3^--N in both periods. In August 2017, the NO_3^--N concentration increased sharply from the epilimnion to the middle layer, and then decreased in the hypolimnion (excluding Site 5). The NH_4^+-N concentration varied slightly with depth, however, an extremely high concentration of NH_4^+-N was observed in the epilimnion at Site 2. The concentrations of TDN and NO_3^--N both changed slightly in the vertical profile in January 2018.

The TDP and SRP concentrations were both below the detectable limit of the colorimetric molybdenum blue method (0.01 mg L^{-1}), and the concentrations of TP in August 2017 and January 2018 were 0.01–0.02 and 0.01–0.04 mg L^{-1}, respectively (Fig. 3k and l). The TDN/TP ratios in the epilimnion were 380–1187 and 160–1051 in August 2017 and January 2018. Therefore, the TDN/TDP ratios would be even higher. The ratio indicates that P is the limiting factor of phytoplankton growth in Hongjiadu Reservoir.

3.3. Contents of particulate C, N, and P

The contents of PTC, PIC, and POC varied from 65.9 to 88.9, 6.73 to 24.3 and 47.1–80.3 mg g^{-1} in August 2017, respectively, and varied from 41.1 to 56.9, 1.39 to 6.93, and 39.0–51.6 mg g^{-1} in January 2018, respectively. POC was the main fraction of PTC in both periods. The contents of PTC and POC both decreased with depth, while that of PIC increased in the stratification period (excluding Site 6). However, all these factors decreased slightly with depth in the mixing period (Fig. 4a and b).

The PTP, PIP, and POP contents ranged from 1.23 to 1.78, 0.65 to 1.24, and 0.36–0.74 mg g^{-1} in August 2017, respectively, while they ranged from 1.84 to 2.38, 0.87 to 1.69, and 0.65–1.24 mg g^{-1} in January 2018, respectively. Generally, the contents of PIP and POP were higher in January 2018. During summer, the contents of PIP increased from the epilimnion to the hypolimnion, while that of POP decreased with depth. Meanwhile, the contents of PTP, PIP, and POP were also less variable in the vertical direction in the mixing period (Fig. 4c and d).

The POC/POP ratios increased from the epilimnion (222–341) to the middle layer (288–367), but declined to the hypolimnion (253–363) in August 2017 (Fig. 4e). In January 2018, the POC/POP ratios varied slightly in the vertical direction (90–183) (Fig. 4f). The POC/PN ratios also increased with depth during August 2017, and varied slightly during January 2018 (Fig. 4g and h). Furthermore, the POC/POP and POC/PN ratios in the epilimnion were both highest at Site 2 in August 2017.

3.4. Contents of Al, Zr, Fe, and Mn in particulates

Among the four elements, the contents of Fe and Al in particulates were highest at both sites, while the content of Zr was lowest (Table 2). In August 2017, the contents of Al and Fe decreased with depth, while the Mn content increased at the two sites. In the hypolimnion, the contents of Al and Fe still remained high. While Zr varied slightly in the vertical profile. The contents of Al, Fe, Mn and Zr were higher in the epilimnion at Site 2 than those at Site 5. In January 2018, the contents of the four metal elements all varied slightly in the vertical direction. Additionally, the contents of Al and Fe were higher in the epilimnion in the stratification period, while the contents of Mn and Zr were lower.

4. Discussion

4.1. Spatial and temporal variations of physical and chemical parameters in water column

The first thermocline could be created by stronger solar radiation providing the surface water with heat, causing it to become more buoyant and preventing exchange with deeper water (Wang et al., 2017). The first thermocline caused the inflowing water to form a density current and flow downwards. The temperature of the inflowing water was higher, causing turbulence to erode the middle layer, which had a lower temperature, forming the second thermocline (Li et al., 2014). The "two thermoclines" could also be formed by wind speed (Branco and Torgersen, 2009), but it was not likely to be the dominant factor. Hongjiadu Reservoir is very deep, and the water depth of every observed site exceeds 120 m. Therefore, the water could not be affected

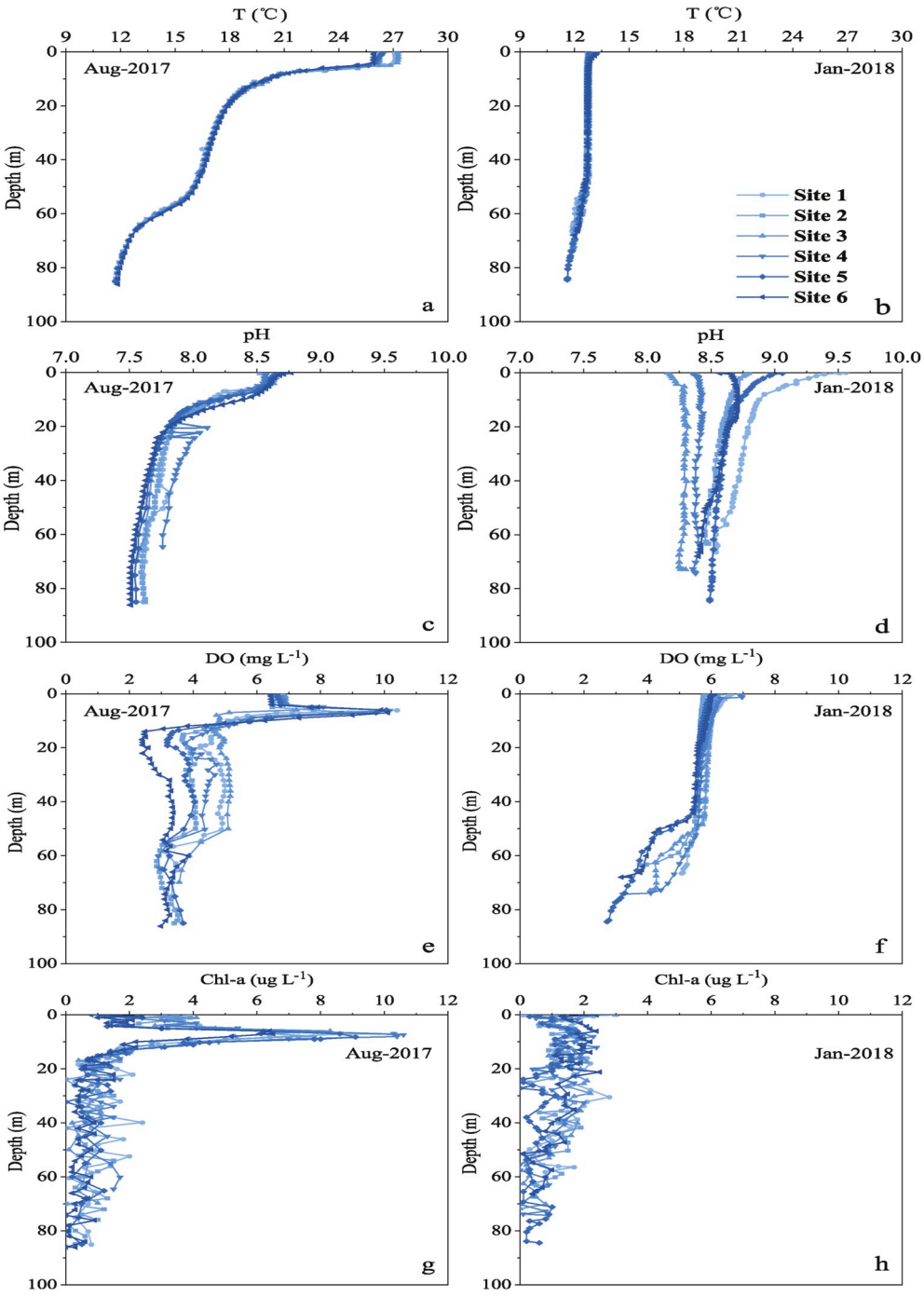

Fig. 2. Seasonal variations of physical and chemical parameters in water column of Hongjiadu Reservoir.

by the wind so strongly to form the second thermocline. Additionally, Hongjiadu Reservoir is surrounded by mountains, which could also limit the wind speed (Zhang et al., 2015).

Two oxyclines were observed (water layer where the DO concentration gradient is > 0.2 mg L^{-1} m^{-1}) in Hongjiadu Reservoir (excluding Site 6). The first oxycline existed at the bottom of the first thermocline, and the other was located in the second thermocline. Zhang et al. (2015) demonstrated that the oxycline depth positively correlated with the thermocline depth, indicating that the thermal stratification pattern strongly affected the stratification of DO in the deep reservoir/lake (Liu et al., 2019). Phytoplankton photosynthesis also influences DO stratification (Zhang et al., 2015). In the epilimnion, the concentrations of Chl-a and DO both peaked at 7–8 m (upper layer of the first thermocline), due to intense photosynthesis. The water transparency of Hongjiadu Reservoir was only 3.1–4.6 m in the stratification period, and lower light availability would limit phytoplankton photosynthesis at the bottom of the first thermocline (Zhou et al., 2019), declining the phytoplankton community size and oxygen content. Additionally, the water densities at the top and bottom of the thermocline are different, organic matter subsides gently and the stagnation time is longer in the thermocline. Therefore, part of easily degradable organic matter would decompose in the thermocline, causing the DO to significantly decline (Chen et al., 2018). Although the parameters of the bottom water were not available, the DO contents at the bottom were likely lower than that at the maximum depth we measured. Furthermore, at Site 6, which was located in front of the dam of Hongjiadu Reservoir, the dam operation

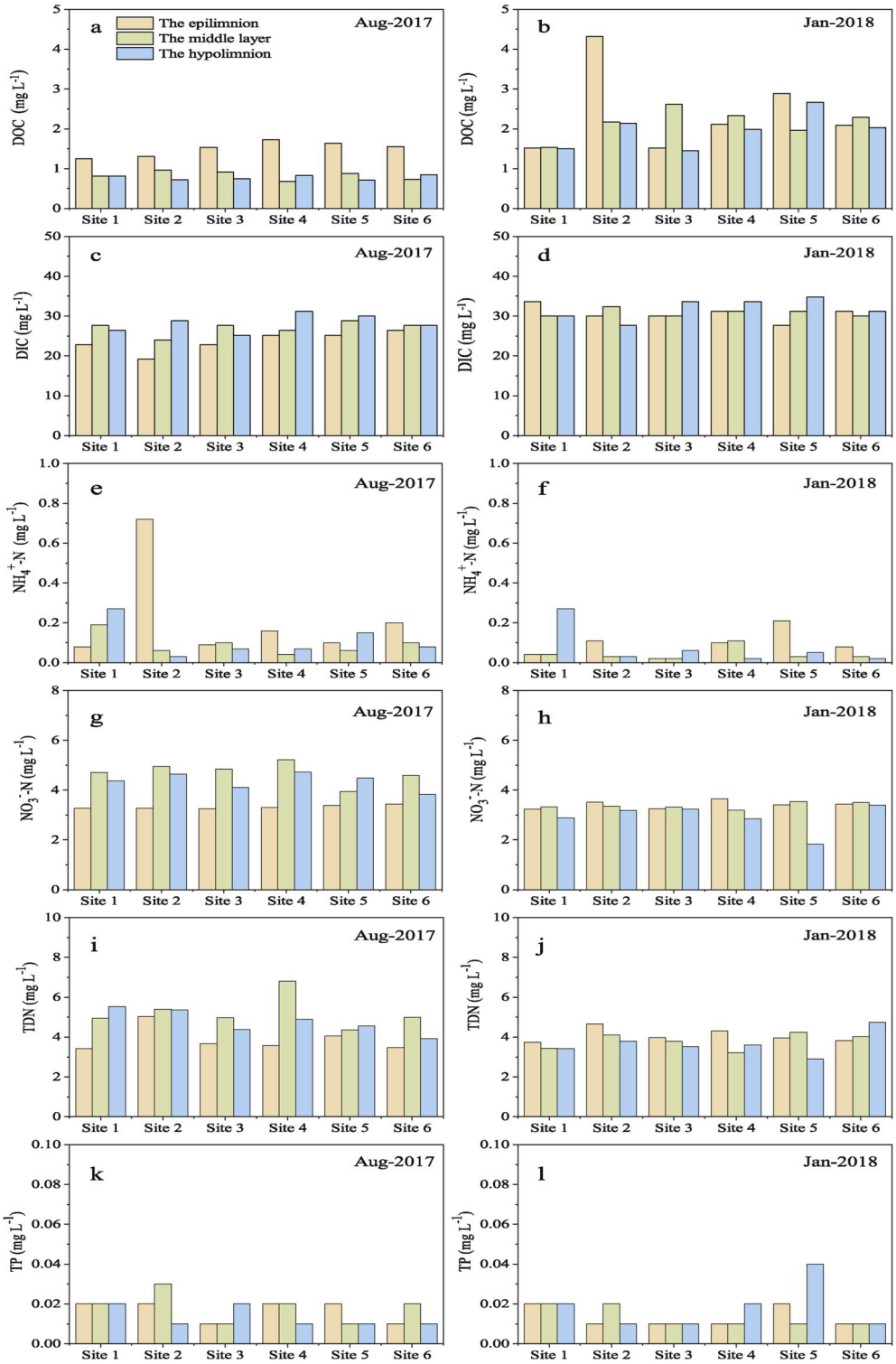

Fig. 3. Spatial distributions of DOC, DIC, NH_4^+-N, NO_3^--N, TDN and TP in August 2017 and January 2018.

would ventilate the water, therefore, the second oxycline did not form at the middle layer in summer.

Double thermoclines have also been observed in Pingzhai Reservoir (data not published), Fuxian Lake, and Songtao Reservoir, indicating that the multi-thermoclines could form in the deep reservoir/lake (Fang et al., 2019). The thermal gradients persist longer in the deep reservoir/lake (Edlund et al., 2017). Along with the bithermocline formation, bioxycline would be generated correspondingly in most cases, leading to the formation of an anoxic environment in the bottom water.

4.2. *Characteristics of C and P during the deposition of particulate matter*

The contents of POC and POP both decreased with depth in the stratification period, indicating that organic matter was degraded during the deposition of particulate matter. From the epilimnion to the middle layer, where the organic matter deposited through the thermocline, organic matter degradation resulted in a dramatic decline in the POC and POP concentrations. The contents of POC and POP decreased by approximately 9% and 15%, respectively, from the epilimnion to the

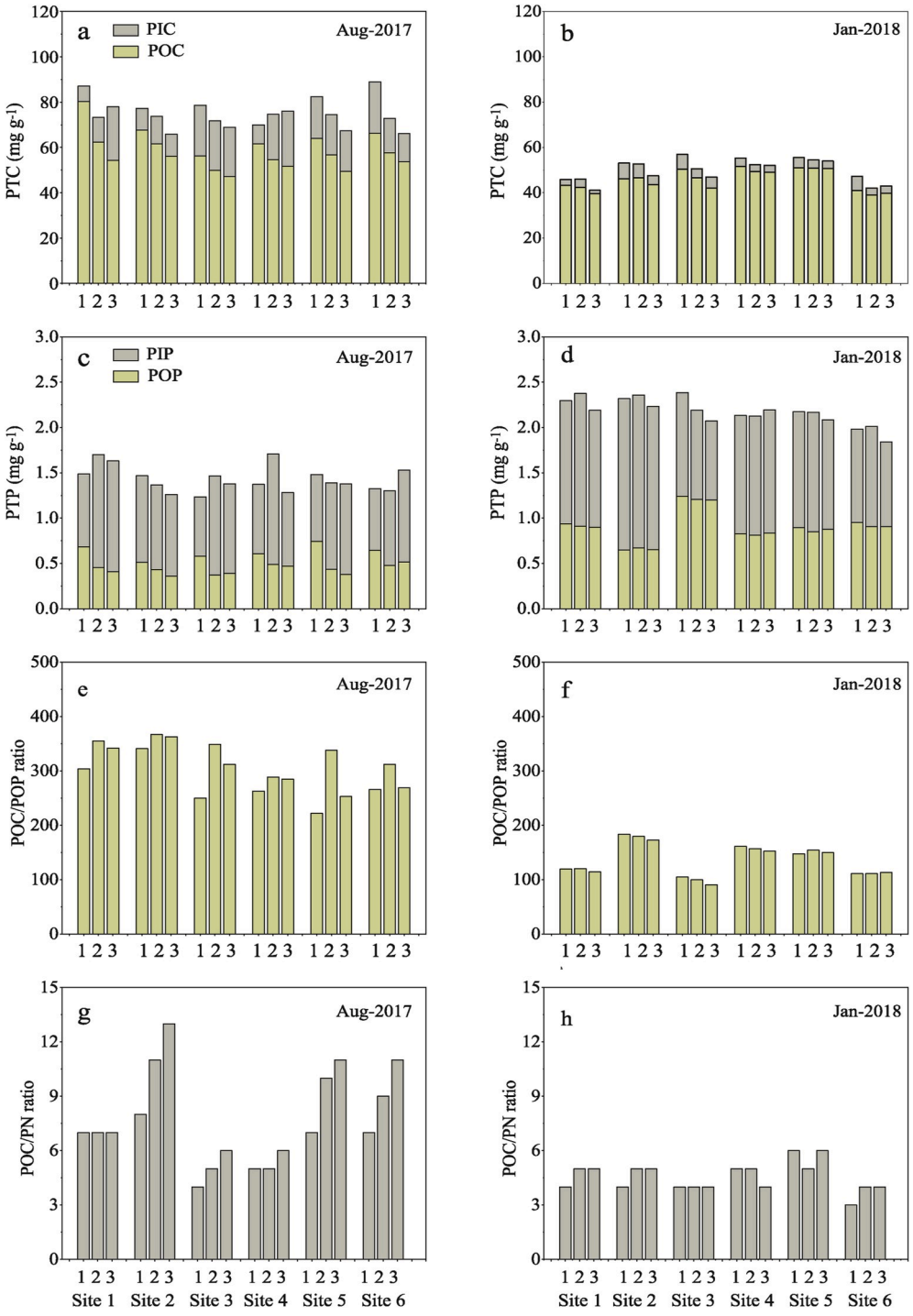

Fig. 4. Spatial distributions of the contents of particulate C, P, and the ratios of POC/POP, POC/PN in August 2017 and January 2018. "1", "2", and "3" represented the epilimnion, the middle layer, and the hypolimnion, respectively.

middle layer at Site 2, while the POC and POP contents at the other sites decreased by approximately 11%–22% and 19%−41% in August 2017, respectively. The higher sedimentation efficiency at Site 2 might result from the higher proportion of terrestrial organic matter, which was less reactive than aquatic organic matter (Ingall et al., 2005).

Phytoplankton photosynthesis utilizes DIC to form organics, while the respiration and degradation of organic matter release DIC and DOC (Murrell and Hollibaugh, 2000; Parker et al., 2010; Chen et al., 2018; Li et al., 2018). Photosynthesis is the dominant process in the epilimnion, which leads to higher primary productivity. Simultaneously, organic matter could decompose into DOC and DIC, but the regeneration of DIC may be lower than its consumption, resulting in higher DOC concentrations and lower DIC concentrations in the epilimnion. Photosynthesis is weaker in deeper water, while the respiration and degradation of organic matter are predominant, so DIC is released into water again. DOC is synchronously mineralized (Kim et al., 2006; Li and Wang, 2011). The lower DOC concentrations in the deep layer indicates that the mineralization rate is greater than production rate there. The NO_3^--N content significantly negatively correlated with the contents of POC, POP, and DOC (Table 3). This phenomenon was also observed in Hongfeng Lake (Li et al., 2008). In the euphotic zone, NO_3^--N is assimilated by algae as a nutrient, while the degradation of dissolved and particulate

Table 2
Contents of Al, Zr, Fe, Mn and the ratio of PTP/Zr, PIP/Zr and POP/Zr in particulate matters at Site 2 and Site 5 in August 2017 and January 2018.

		Al (ug g^{-1})	Zr (ug g^{-1})	Fe (ug g^{-1})	Mn (ug g^{-1})	PTP/Zr ratio	PIP/Zr ratio	POP/Zr ratio
Site 2 (Aug 2017)	Epilimnion	11140	58	13772	349	25	16	9
	Middle layer	10828	53	11241	501	26	17	8
	Hypolimnion	9709	53	9647	728	24	17	7
Site 5 (Aug 2017)	Epilimnion	10126	50	11802	260	30	15	15
	Middle layer	9491	49	10920	449	28	19	9
	Hypolimnion	8348	51	10049	557	27	20	7
Site 2 (Jan 2018)	Epilimnion	9073	62	10043	441	37	26	10
	Middle layer	9287	62	9312	504	38	27	11
	Hypolimnion	8642	58	9609	449	38	27	11
Site 5 (Jan 2018)	Epilimnion	8556	68	8208	442	32	19	13
	Middle layer	8774	65	8665	472	33	20	13
	Hypolimnion	8161	66	8444	501	31	18	13

organic matter releases NO_3^--N into deeper water. Additionally, owing to the thermal stratification, the deeper water is not likely to well up, leading to the increase of the DIC and NO_3^--N contents there.

The contents of particulate and dissolved C and P all varied slightly in the water column in the mixing period. In winter, the temperature is lower and the cold surface water could not sustain phytoplankton in the photic zone, limiting the growth of phytoplankton (Sommer, 1985). The lower phytoplankton biomass and external influx result in the lower contents of POC, PIC, and Chl-a, and higher water transparency. The slight variations of the contents of particulate and dissolved C and P in vertical profiles are due to vertical mixing and the lower availability of microorganisms (Wang et al., 2017). Microbial respiration and the sinking velocity of particulates could be the main factors controlling the sedimentation efficiency of particulate matter (De La Rocha and Passow, 2007; Trull et al., 2008; Mcdonnell et al., 2015). The sinking velocity is higher due to the intensive hydrodynamics, and microbial respiration is lower due to the lower temperature in the mixing period (Gudasz et al., 2010; Toseland et al., 2013). The sedimentation efficiencies of POC and POP were 79 ± 6% and 68 ± 10% respectively in the stratification period, while they were 94 ± 5% and 98 ± 2% respectively in the mixing period in Hongjiadu Reservoir.

The contents of PTP and POP in the stratification period were lower than those in the mixing period, which was likely due to the higher proportion of coarse particles, such as sand, in the particulate matters in August 2017. Heavy rainfall could cause more coarse particles from the catchment to enter lakes/reservoirs. Xiong et al. (2008) also found that the sand quantity positively correlated with rainfall in Wujiang Basin, and the coarse particles contained lower P contents (Yang et al., 2019). Therefore, the lower contents of PTP and POP in August 2017 were likely due to the dilution of coarse terrigenous matter input.

4.3. Variations of POC/POP ratios in both periods

The intense photosynthesis in summer increases the phytoplankton biomass, while the SRP amount is insufficient to support phytoplankton growth. Therefore, the phytoplankton would utilize phosphatase to hydrolyze the cellular phosphorus for sustenance (Wang et al., 2018). This results in higher POC/POP ratios in summer (Fig. 4e and f). In winter, the moderate photosynthesis results in a lower POC content (Fig. 4a and b), and the phosphatase activity is lower due to the lower temperature (Chuai et al., 2011). The organic matter source also affects the POC/POP ratio (Ingall and Vancappellen, 1990), but it is not the dominant factor, as the POC/PN ratios were all below 10 in the epilimnion, suggesting that organic matter came mainly from phytoplankton in the two periods (Meyers, 1994).

The POC/POP ratios also increased with depth in the stratification period (Fig. 4e), particularly from the epilimnion to the middle layer, indicating that P was preferentially regenerated relative to C during organic matter decomposition. This phenomenon is consistent with that observed in previous studies conducted in the marine ecosystem (Bishop et al., 1978; Knauer et al., 1979). However, the ratios declined slightly from the middle layer to the hypolimnion, which might be attributed to the intense decomposition of the fraction of easily decomposed organic matter (Ingall and Jahnke, 1997; Jilbert et al., 2011). This is supported by the slight decline in the contents of POC and POP.

4.4. Transformation of particulate P in the stratification period

POP decreased during organic matter decomposition in the stratification period, but the concentrations of DTP and SRP were still below 0.01 mg L^{-1}. On the contrary, the content of PIP increased with increasing depth (Fig. 4c). Organic matter degradation declines the net mass of particulate matters, which may result in higher contents of PIP. In order to estimate the influence of organic matter degradation on the PIP contents, the Zr content was used to standardize the PIP contents. The PIP/Zr ratios increased with depth in the stratification period (Table 2), indicating that the increase of PIP with depth was not caused by the lower mass. Additionally, there was a significant negative correlation between PIP and POP ($R^2 = 0.387$, $p < 0.01$), indicating that POP transformed into PIP in deeper water. The physiological status of

Table 3
Pearson's correlation coefficients (R) of dissolved and particulate C, N and P in August 2017.

	DOC	DIC	NO_3^--N	NH_4^+N	DTN	TP	POC	PIC	POP	PIP
DOC	1									
DIC	- 0.559[b]	1								
NO_3^--N	- 0.820[a]	0.572[b]	1							
NH_4^+-N	0.258	- 0.565[b]	- 0.357	1						
DTN	0.613[a]	0.260	0.573[b]	0.106	1					
TP	0.221	- 0.516[b]	0.102	0.172	- 0.044	1				
POC	0.563[b]	- 0.585[b]	- 0.544[b]	0.303	- 0.392	0.367	1			
PIC	- 0.136	0.344	0.221	- 0.200	0.271	- 0.361	- 0.596[a]	1		
POP	0.823[a]	- 0.448	- 0.732[a]	0.068	- 0.461	0.139	0.708[a]	- 0.173	1	
PIP	- 0.694[a]	0.210	0.639[a]	0.100	0.592[a]	0.191	- 0.354	0.035	- 0.622[a]	1

[a] Correlation was significant at the 0.01 level.
[b] Correlation was significant at the 0.05 level.

phytoplankton may influence the proportion of PIP (Yoshimura et al., 2018). In the epilimnion, the intense photosynthesis accelerates phytoplankton growth, resulting in higher POP/PTP ratios. Organic matter degradation is the main process in deeper water, with some enzymes (such as alkaline phosphatase) contributing to the mineralization of POP to phosphate. Furthermore, the influx of external soils containing metal hydroxides minerals (Di et al., 2015), which could adsorb PO_4^{3-} under oxic conditions (Sanudo-Wilhelmy et al., 2004; Fu et al., 2005; Wang et al., 2019b), may lead to an increase in the PIP content. However, these redox-sensitive phosphorus would be released in the hypoxic water environment (Gomez et al., 1999).

4.5. Potential risk of nutrient release in the large deep reservoir

Two thermoclines exist in Hongjiadu Reservoir in the stratification period, leading to low DO concentration in the hypolimnion, even though the oxygen consumption of the water is not very high at present. If the hypolimnion environment is hypoxic, P would be released. For example, $Fe(OH)_3$ could be reduced into $Fe(OH)_2$, which is soluble under hypoxic conditions, leading to the regeneration of inorganic phosphorus from particulates (Fan et al., 2006). The POC/POP ratio demonstrates that POP is preferentially regenerated relative to POC in the stratification period. P is the limiting factor of phytoplankton growth in Hongjiadu Reservoir. Therefore, the release of P would enhance primary productivity. The greater primary productivity increases the oxygen demand, further reducing the DO content in water column (Ingall et al., 1993; Zhu et al., 2013). If the water becomes hypoxic, the release of P from the particulates and sediments into the water would be stimulated, further increasing the primary productivity, such as in Lake Soyang (Korea) (Kim et al., 2016) and Fei-Tsui Reservoir (Taiwan) (Chen and Wu, 2003). This positive feedback may accelerate P recycling and sustain water eutrophication in large deep reservoirs. Once if eutrophication occurs in these reservoirs, it will be very difficult to restore the water ecosystem. Thus, it is particularly important to prevent the occurrence of eutrophication and the formation of positive feedback loop as early as possible. Firstly, the external input of nutrients should be strictly controlled to prevent eutrophication. Secondly, the rational operation of reservoir is helpful to weaken the stability of stratification and improve the DO level of the bottom water. Besides, aeration/oxygenation is also an effective way to increase DO of bottom water (Huang et al., 2014). In the stratification period, the bottom water can be aerated/oxygenated to improve the DO level so as to prevent P release in the bottom water and sediments. In addition, the Palladium based nanoparticle catalysts, which can effectively reduce nitrite and nitrate and selectively produce N_2 (Guo et al., 2017; Li et al., 2019a), also provide a promising way to reduce primary productivity in the N-replete reservoirs.

5. Conclusion

The contents of both POC and POP decreased with depth in summer, indicating that organic matter was degraded during the deposition of particulate matter. The POC/POP ratios were lower in the epilimnion and increased with depth, suggesting that P was preferentially regenerated relative to C during organic matter degradation. However, the contents of POC and POP varied slightly with depth in winter. The thermal stratification in summer is the main cause of this difference. Solar radiation and the warm inflowing water cause the formation of bithermocline and bioxycline in the water column in Hongjiadu Reservoir in the stratification period. The PIP content and PIP/Zr ratio increased with depth in summer, and the contents of PIP and POP were significantly negatively correlated. This indicates that POP transformed into PIP in deeper water.

The bithermocline and bioxycline impede the upper and bottom water exchange and result in low DO concentrations in the hypolimnion in Hongjiadu Reservoir. If the water becomes hypoxic, enhanced P release during organic matter degradation will promote phytoplankton growth, leading to higher phytoplankton biomass and more severe DO depletion in the bottom water. Thus, a positive feedback loop would form among hypoxia, enhanced P release, higher primary productivity and more severe hypoxia in large deep lakes/reservoirs, like Hongjiadu Reservoir. This positive feedback may accelerate P recycling and sustain water eutrophication in large deep reservoirs. Once if eutrophication occurs in these reservoirs, it will be very difficult to restore the water ecosystem. Thus, it is particularly important to prevent the occurrence of eutrophication and the formation of positive feedback loop as early as possible. This highlights the importance of both reducing external loading and improving DO level in large deep reservoirs.

Declaration of competing interest

All authors have read and approved this version of the article, and no conflict of interest exits in the submission of this manuscript. This manuscript has not been published or presented elsewhere in part or in whole, and it is not under consideration by another journal.

CRediT authorship contribution statement

Jia Yu: Investigation, Formal analysis, Data curation, Writing - original draft. **Jingan Chen:** Conceptualization, Methodology, Writing - review & editing, Project administration. **Yan Zeng:** Conceptualization, Methodology, Writing - review & editing. **Yaoting Lu:** Investigation, Formal analysis, Data curation. **Quan Chen:** Investigation, Formal analysis.

Acknowledgements

This work was financially supported by the National Key Research and Development Project of China (grant number 2016YFA0601003); and the National Natural Science Foundation of China (grant numbers U1612441, 41573137).

References

Ahlgren, J., Tranvik, L., Gogoll, A., Waldeback, M., Markides, K., Rydin, E., 2005. Sediment depth attenuation of biogenic phosphorus compounds measured by P-31 NMR. Environ. Sci. Technol. 39, 867–872. https://doi.org/10.1021/es049590h.

Aspila, K.I., Agemian, H., Chau, A.S.Y., 1976. Semiautomated method for determination of inorganic, organic and total phosphate in sediments. Analyst 101, 187–197. https://doi.org/10.1039/an9760100187.

Baldwin, D.S., 2013. Organic phosphorus in the aquatic environment. Environ. Chem. 10, 439–454. https://doi.org/10.1071/en13151.

Bao, L.L., Li, X.Y., Cheng, P., 2018. Phosphorus retention along a typical urban landscape river with a series of rubber dams. J. Environ. Manag. 228, 55–64. https://doi.org/10.1016/j.jenvman.2018.09.019.

Bishop, J.K.B., Ketten, D.R., Edmond, J.M., 1978. Chemistry, biology and vertical flux of particulate matter from the upper 400m of the cape basin in the Southeast Atlantic Ocean. Deep-Sea Res. 25, 1121–1161. https://doi.org/10.1016/0146-6291(78)90010-3.

Branco, B.F., Torgersen, T., 2009. Predicting the onset of thermal stratification in shallow inland waterbodies. Aquat. Sci. 71, 65–79. https://doi.org/10.1007/s00027-009-8063-3.

Chen, Y.J., Wu, S.C., 2003. Effects of sediment phosphorus release associated with the density current on water quality of a subtropical and deep reservoir in Taiwan. Water Sci. Technol. 48, 151–158.

Chen, C.Y., Liu, Z.H., 2017. The role of biological carbon pump in the carbon sink and water environment improvement in karst surface aquatic ecosystems. Chin. Sci. Bull. 62, 3440–3450. https://doi.org/10.1360/N972017-00298.

Chen, J.A., Yang, H.Q., Zeng, Y., Guo, J.Y., Song, Y.L., Ding, W., 2018. Combined use of radiocarbon and stable carbon isotope to constrain the sources and cycling of particulate organic carbon in a large freshwater lake, China. Sci. Total Environ. 625, 27–38. https://doi.org/10.1016/j.scitotenv.2017.12.275.

Chen, J.A., Zeng, Y., Yu, J., Wang, J.F., Yang, H.Q., Lu, Y.T., 2019. Preferential regeneration of P relative to C in a freshwater lake. Chemosphere 222, 15–21. https://doi.org/10.1016/j.chemosphere.2019.01.088.

Chuai, X.M., Ding, W., Chen, X.F., Wang, X.L., Miao, A.J., Xi, B.D., He, L.S., Yang, L.Y., 2011. Phosphorus release from cyanobacterial blooms in meiliang bay of lake taihu, China. Ecol. Eng. 37, 842–849. https://doi.org/10.1016/j.ecoleng.2011.01.001.

De La Rocha, C.L., Passow, U., 2007. Factors influencing the sinking of POC and the efficiency of the biological carbon pump. Deep-Sea Res. Part II. 54, 639–658. https://doi.org/10.1016/j.dsr2.2007.01.004.

Di, X.Y., An, X.J., Dong, H., Tang, H.M., Xiao, B.H., 2015. The distribution and evolution of soil organic matter in the Karst Region, Guizhou Province, Southwestern China. Earth Environ. 43, 697–708. https://doi.org/10.14050/j.cnki.1672-9250.2015.06.014.

Dijkstra, N., Kraal, P., Seguret, M.J.M., Flores, M.R., Gonzalez, S., Rijkenberg, M.J.A., Slomp, C.P., 2018. Phosphorus dynamics in and below the redoxcline in the Black Sea and implications for phosphorus burial. Geochem. Cosmochim. Acta 222, 685–703. https://doi.org/10.1016/j.gca.2017.11.016.

Edlund, M.B., Almendinger, J.E., Fang, X., Hobbs, J.M.R., VanderMeulen, D.D., Key, R.L., Engstrom, D.R., 2017. Effects of climate change on lake thermal structure and biotic response in Northern Wilderness Lakes. Water 9. https://doi.org/10.3390/w9090678.

Fan, C.X., Zhang, L., Bao, X.M., You, B.S., Zhong, J.C., Wang, J.J., Ding, S.M., 2006. Migration mechanism of biogenic elements and their quantification on the sediment water interface of Lake Taihu: II.chemical thermodynamic mechanism of phosphorus release and its source-sink transition. J. Lake Sci. 18, 207–217.

Fang, Q., Ma, J.B., Shen, W.L., Xiong, S., Lu, B.H., 2019. Study on numerical simulation of water temperature in Songtao Reservoir. Hydroelectr. Power 1–9.

Fu, F.X., Zhang, Y.H., Leblanc, K., Sanudo-Wilhelmy, S.A., Hutchins, D.A., 2005. The biological and biogeochemical consequences of phosphate scavenging onto phytoplankton cell surfaces. Limnol. Oceanogr. 50, 1459–1472. https://doi.org/10.4319/lo.2005.50.5.1459.

Gao, Y., Wang, B.L., Lin, X.L., Wang, Y.C., Zhang, J., Jiang, Y.X., Wang, F.S., 2013. Impacts of river impoundment on the riverine water chemistry composition and their response to chemical weathering rate. Front. Earth Sci. 7, 351–360. https://doi.org/10.1007/s11707-013-0366-y.

Gomez, E., Durillon, C., Rofes, G., Picot, B., 1999. Phosphate adsorption and release from sediments of brackish lagoons: pH, O_2 and loading influence. Water Res. 33, 2437–2447. https://doi.org/10.1016/s0043-1354(98)00468-0.

Gudasz, C., Bastviken, D., Steger, K., Premke, K., Sobek, S., Tranvik, L.J., 2010. Temperature-controlled organic carbon mineralization in lake sediments. Nature 466, 478. https://doi.org/10.1038/nature09186.

Guo, S.J., Heck, K., Kasiraju, S., Zhao, Z., Grabow, L.C., Miller, J.T., Wong, M.S., 2017. Insights into nitrate reduction over indium-decorated palladium nanoparticle catalysts. ACS Catal. 8, 503–515. https://doi.org/10.1021/acscatal.7b01371.

Han, W.Y., Wang, M.B., Wang, H.K., 1994. The vertical carbon flux of epipelagic water in the Nansha Area of the South China Sea. Oceanol. Limnol. Sinica 3, 345–348.

He, R.R., Gao, Y.X., Wang, F., Zhu, G.W., Chen, W.M., 2009. Spatial-temporal distribution of nutrients and its causation in Tianmu Lake, China. J. Agro-Environ. Sci. 28, 353–360.

Hedges, J.I., Stern, J.H., 1984. Carbon and nitrogen determinations of carbonate-containing solids. Limnol. Oceanogr. 29, 657–663. https://doi.org/10.4319/lo.1984.29.3.0657.

Huang, T.L., Ma, Y., Cong, H.B., Tan, P., 2014. Application of the technology of water lifting and aeration on improving water quality in a Deep Canyon Reservoir - a case study from northern China. Desalin. Water Treat 52, 1636–1646. https://doi.org/10.1080/19443994.2013.848680.

Ingall, E.D., Vancappellen, P., 1990. Relation between sedimentation-rate and burial of organic phosphorus and organic carbon in marine sediments. Geochem. Cosmochim. Acta 54, 373–386. https://doi.org/10.1016/0016-7037(90)90326-g.

Ingall, E.D., Bustin, R.M., Vancappellen, P., 1993. Influence of water column anoxia on the burial and preservation of carbon and phosphorus in marine shales. Geochem. Cosmochim. Acta 57, 303–316. https://doi.org/10.1016/0016-7037(93)90433-w.

Ingall, E., Jahnke, R., 1997. Influence of water-column anoxia on the elemental fractionation of carbon and phosphorus during sediment diagenesis. Mar. Geol. 139, 219–229. https://doi.org/10.1016/s0025-3227(96)00112-0.

Ingall, E., Kolowith, L., Lyons, T., Hurtgen, M., 2005. Sediment carbon, nitrogen and phosphorus cycling in an anoxic fjord, Effingham Inlet. British Columbia. Am. J. Sci. 305, 240–258. https://doi.org/10.2475/ajs.305.3.240.

Jilbert, T., Slomp, C.P., Gustafsson, B.G., Boer, W., 2011. Beyond the Fe-P-redox connection: preferential regeneration of phosphorus from organic matter as a key control on Baltic Sea nutrient cycles. Biogeosciences 8, 1699–1720. https://doi.org/10.5194/bg-8-1699-2011.

Joshi, S.R., Kukkadapu, R.K., Burdige, D.J., Bowden, M.E., Sparks, D.L., Jaisi, D.P., 2015. Organic matter remineralization predominates phosphorus cycling in the mid-bay sediments in the Chesapeake Bay. Environ. Sci. Technol. 49, 5887–5896. https://doi.org/10.1021/es5059617.

Kim, C., Nishimura, Y., Nagata, T., 2006. Role of dissolved organic matter in hypolimnetic mineralization of carbon and nitrogen in a large, monomictic lake. Limnol. Oceanogr. 51, 70–78. https://doi.org/10.4319/lo.2006.51.1.0070.

Kim, K., Kim, B., Knorr, K.H., Eum, J., Choi, Y., Jung, S., Peiffer, S., 2016. Potential effects of sediment processes on water quality of an artificial reservoir in the Asian monsoon region. Inland Waters 6, 423–435. https://doi.org/10.5268/iw-6.3.852.

Knauer, G.A., Martin, J.H., Bruland, K.W., 1979. Fluxes of particulate carbon, nitrogen, and phosphorus in the upper water column of the Northeast Pacific. Deep-Sea Res. 26, 97–108. https://doi.org/10.1016/0198-0149(79)90089-x.

Komada, T., Anderson, M.R., Dorfmeier, C.L., 2008. Carbonate removal from coastal sediments for the determination of organic carbon and its isotopic signatures, delta C-13 and delta C-14: comparison of fumigation and direct acidification by hydrochloric acid. Limnol Oceanogr. Methods 6, 254–262. https://doi.org/10.4319/lom.2008.6.254.

Li, W., Wu, F.C., Liu, C.Q., Fu, P.Q., Wang, J., Mei, Y., Wang, L.Y., Guo, J.Y., 2008. Temporal and spatial distributions of dissolved organic carbon and nitrogen in two small lakes on the Southwestern China Plateau. Limnology 9, 163–171. https://doi.org/10.1007/s10201-008-0241-9.

Li, N., Wang, J.T., 2011. Dissolved inorganic and organic carbon in the North of East China Sea (ECS) coastal waters in spring. Mar. Sci.. (Beijing, China) 35, 5–10.

Li, J., Liang, R.F., Deng, Y., Tuo, Y.C., 2014. Flow field of thermally stratified reservoir. J. Tianjin Univ. Sci. Technol. 47, 395–400. https://doi.org/10.11784/tdxbz201209046.

Li, Z.C., Zhao, Y.P., Xu, X.G., Han, R.M., Wang, M.Y., Wang, G.X., 2018. Migration and transformation of dissolved carbon during accumulated cyanobacteria decomposition in shallow eutrophic lakes: a simulated microcosm study. Peerj 6. https://doi.org/10.7717/peerj.5922.

Li, H., Guo, S.J., Shin, K., Wong, M.S., Henkelman, G., 2019a. Design of a Pd-Au nitrite reduction catalyst by identifying and optimizing active ensembles. ACS Catal. 9, 7957–7966. https://doi.org/10.1021/acscatal.9b02182.

Li, W.N., Wang, X.X., Cai, H., Li, X.N., Zhao, X.J., Mei, Y.D., 2019b. Emergy transformity of river in complex river. China Environ. Sci. 39, 5094–5100. https://doi.org/10.19674/j.cnki.issn1000-6923.20190929.001.

Liu, X.L., Liu, C.Q., Li, S.L., Wang, F.S., Wang, B.L., Wang, Z.L., 2011. Spatiotemporal variations of nitrous oxide (N_2O) emissions from two reservoirs in SW China. Atmos. Environ. 45, 5458–5468. https://doi.org/10.1016/j.atmosenv.2011.06.074.

Liu, M., Zhang, Y.L., Shi, K., Zhu, G.W., Wu, Z.X., Liu, M.L., Zhang, Y.B., 2019. Thermal stratification dynamics in a large and deep subtropical reservoir revealed by high-frequency buoy data. Sci. Total Environ. 651, 614–624. https://doi.org/10.1016/j.scitotenv.2018.09.215.

Maavara, T., Parsons, C.T., Ridenour, C., Stojanovic, S., Durr, H.H., Powley, H.R., Van Cappellen, P., 2015. Global phosphorus retention by river damming. Proc. Natl. Acad. Sci. U.S.A. 112, 15603–15608. https://doi.org/10.1073/pnas.1511797112.

Maavara, T., Chen, Q., Van Meter, K., Brown, L.E., Zhang, J.Y., Ning, J.R., Zarfl, C., 2020. River dam impacts on biogeochemical cycling. Nat Rev Earth Environ 1, 103–116. https://doi.org/10.1038/s43017-019-0019-0.

Mcdonnell, A.M.P., Boyd, P.W., Buesseler, K.O., 2015. Effects of sinking velocities and microbial respiration rates on the attenuation of particulate carbon fluxes through the mesopelagic zone. Global Biogeochem. Cycles 29, 175–193. https://doi.org/10.1002/2014GB004935.

Meyers, P.A., 1994. Preservation of elemental and isotopic source identification of sedimentary organic-matter. Chem. Geol. 114, 289–302. https://doi.org/10.1016/0009-2541(94)90059-0.

Murrell, M.C., Hollibaugh, J.T., 2000. Distribution and composition of dissolved and particulate organic carbon in northern San Francisco Bay during low flow conditions. Estuar. Coast Shelf Sci. 51, 75–90. https://doi.org/10.1006/ecss.2000.0639.

Parker, S.R., Gammons, C.H., Poulson, S.R., DeGrandpre, M.D., Weyer, C.L., Smith, M.G., Babcock, J.N., Oba, Y., 2010. Diel behavior of stable isotopes of dissolved oxygen and dissolved inorganic carbon in rivers over a range of trophic conditions, and in a mesocosm experiment. Chem. Geol. 269, 22–32. https://doi.org/10.1016/j.chemgeo.2009.06.016.

Reitzel, K., Ahlgren, J., Debrabandere, H., Waldeback, M., Gogoll, A., Tranvik, L.J., Rydin, E., 2007. Degradation rates of organic phosphorus in lake sediment. Biogeochemistry 82, 15–28. https://doi.org/10.1007/s10533-006-9049-z.

Roden, E.E., Tuttle, J.H., Boynton, W.R., Kemp, W.M., 1995. Carbon cycling in mesohaline Chesapeake Bay sediments 1: POC deposition rates and mineralization pathways. J. Mar. Res. 53, 799–819.

Rydin, E., 2000. Potentially mobile phosphorus in Lake Erken sediment. Water Res. 34, 2037–2042. https://doi.org/10.1016/s0043-1354(99)00375-9.

Sanudo-Wilhelmy, S.A., Tovar-Sanchez, A., Fu, F.X., Capone, D.G., Carpenter, E.J., Hutchins, D.A., 2004. The impact of surface-adsorbed phosphorus on phytoplankton Redfield stoichiometry. Nature 432, 897–901. https://doi.org/10.1038/nature03125.

Sommer, U., 1985. Seasonal succession of phytoplankton in lake constance. Bioscience 35, 351–357. https://doi.org/10.2307/1309903.

Toseland, A., Daines, S.J., Clark, J.R., Kirkham, A., Strauss, J., Uhlig, C., Lenton, T.M., Valentin, K., Pearson, G.A., Moulton, V., Mock, T., 2013. The impact of temperature on marine phytoplankton resource allocation and metabolism. Nat. Clim. Change 3, 979–984. https://doi.org/10.1038/nclimate1989.

Trull, T.W., Bray, S.G., Buesseler, K.O., Lamborg, C.H., Manganini, S., Moy, C., Valdes, J., 2008. In situ measurement of mesopelagic particle sinking rates and the control of carbon transfer to the ocean interior during the Vertical Flux in the Global Ocean (VERTIGO) voyages in the North Pacific. Deep-Sea Res. Part II. 55, 1684–1695. https://doi.org/10.1016/j.dsr2.2008.04.021.

Van Mooy, B.A.S., Fredricks, H.F., Pedler, B.E., Dyhrman, S.T., Karl, D.M., Koblizek, M., Lomas, M.W., Mincer, T.J., Moore, L.R., Moutin, T., Rappe, M.S., Webb, E.A., 2009. Phytoplankton in the ocean use non-phosphorus lipids in response to phosphorus scarcity. Nature 458, 69–72. https://doi.org/10.1038/nature07659.

Wang, J.F., Chen, J.A., Zeng, Y., Yang, Y.Q., Yang, H.Q., 2012. Spatial distribution characteristics of phosphorus forms in sediment of Lake Hongfeng, Guizhou Province. J. Lake Sci. 24, 789–796.

Wang, L.Y., Zhang, R.Y., Chen, J.A., 2017. Physicochemical characteristics of the overlying water and spatial-temporal distribution of carbon, nitrogen and silicon in Lake Hongfeng, Guizhou Province, China. Earth Environ. 45, 383–389. https://doi.org/10.14050/j.cnki.1672-9250.2017.04.001.

Wang, S.Y., Xiao, J., Wan, L.L., Zhou, Z.J., Wang, Z.C., Song, C.L., Zhou, Y.Y., Cao, X.Y., 2018. Mutual dependence of nitrogen and phosphorus as key nutrient elements: one facilitates dolichospermum flos-aquae to overcome the limitations of the other. Environ. Sci. Technol. 52, 5653–5661. https://doi.org/10.1021/acs.est.7b04992.

Wang, Y.M., Li, K.F., Liang, R.F., Han, S.Q., Li, Y., 2019a. Distribution and release characteristics of phosphorus in a reservoir in Southwest China. Int. J. Environ. Res. Publ. Health 16, 303. https://doi.org/10.3390/ijerph16030303.

Wang, Z.C., Huang, S., Li, D.H., 2019b. Decomposition of cyanobacterial bloom contributes to the formation and distribution of iron-bound phosphorus (Fe-P): insight for cycling mechanism of internal phosphorus loading. Sci. Total Environ. 652, 696–708. https://doi.org/10.1016/j.scitotenv.2018.10.260.

Wu, F.C., Jin, C.X., Zhang, R.Y., Liao, H.Q., Wang, S.R., Jiang, X., Wang, L.Y., Guo, J.Y., Li, W., Zhao, X.L., 2010. Effects and significance of organic nitrogen and phosphorous in the lake aquatic environment. J. Lake Sci. 22, 1–7.

Xiang, P., Wang, S.L., Lu, W.Q., Yang, Y.X., Huang, Q.S., 2016. Distribution and retention efficiency of nitrogen and phosphorus in cascade reservoirs in Wujiang River Basin. Earth Environ. 44, 492–501. http://doi.org/10.14050/j.cnki.1672-9250.2016.05.002.

Xiong, Y.L., Zhang, K.L., Yang, G.X., Gu, Z.K., 2008. Change in characteristics of runoff and sediment in the Wujiang River. Ecol. Environ. 17, 1942–1947. https://doi.org/10.16258/j.cnki.1674-5906.2008.05.055.

Yan, X.C., Wang, M.Y., Xu, X.G., Wang, G.X., Sun, H., Yang, Y.H., Shi, A., 2018. Migration of carbon,nitrogen and phosphorus during organic matter mineralization in eutrophic lake sediments. J. Lake Sci. 30, 306–313. https://doi.org/10.18307/2018.0203.

Yang, B., Zhou, J.B., Lu, D.L., Dan, S.F., Zhang, D., Lan, W.L., Kang, Z.J., Ning, Z.M., Cui, D.Y., 2019. Phosphorus chemical speciation and seasonal variations in surface sediments of the Maowei Sea, northern Beibu Gulf. Mar. Pollut. Bull. 141, 61–69. https://doi.org/10.1016/j.marpolbul.2019.02.023.

Yoshimura, T., Nishioka, J., Ogawa, H., Tsuda, A., 2018. Dynamics of particulate and dissolved organic and inorganic phosphorus during the peak and declining phase of an iron-induced phytoplankton bloom in the eastern subarctic Pacific. J. Mar. Syst. 177, 1–7. https://doi.org/10.1016/j.jmarsys.2017.09.004.

Zhang, Y.L., Wu, Z.X., Liu, M.L., He, J.B., Shi, K., Zhou, Y.Q., Wang, M.Z., Liu, X.H., 2015. Dissolved oxygen stratification and response to thermal structure and long-term climate change in a large and deep subtropical reservoir (Lake Qiandaohu, China). Water Res. 75, 249–258. https://doi.org/10.1016/j.watres.2015.02.052.

Zhou, Q.C., Wang, W.L., Huang, L.C., Zhang, Y.L., Qin, J., Li, K.D., Chen, L., 2019. Spatial and temporal variability in water transparency in Yunnan Plateau lakes, China. Aquat. Sci. 81 https://doi.org/10.1007/s00027-019-0632-5.

Zhu, M.Y., Zhu, G.W., Zhao, L.L., Yao, X., Zhang, Y.L., Gao, G., Qin, B.Q., 2013. Influence of algal bloom degradation on nutrient release at the sediment-water interface in Lake Taihu, China. Environ. Sci. Pollut. Res. 20, 1803–1811. https://doi.org/10.1007/s11356-012-1084-9.

Zhu, Y.R., Feng, W.Y., Liu, S.S., He, Z.Q., Zhao, X.L., Liu, Y., Guo, J.Y., Giesy, J.P., Wu, F. C., 2018. Bioavailability and preservation of organic phosphorus in lake sediments: insights from enzymatic hydrolysis and (31)P nuclear magnetic resonance. Chemosphere 211, 50–61. https://doi.org/10.1016/j.chemosphere.2018.07.134.